Table II. IGLO ^{13}C NMR Chemical Shifts (vs CH_4) for 2-Butyl Cation Isomers

descriptn	IGLO basis//geometry level	angle[a] $C_2^+-C_3-C_4$	$\delta(^{13}C)$ C_1	C_2	C_3	C_4	$(C_1C_4)_{av}$[b]	$(C_2C_3)_{av}$[c]
open chain (3) (classical)	DZ//6-31G*	116.7	45.5	360.8	52.3	7.8	26.7	206.6
methyl bridged (1)	DZ//6-31G*	102.4	43.5	335	49.1	9.3	26.4	192.1
	II'//6-31G*[d]		39.2	338	48.1	5.2	22.2	193.1
	DZ//3-21G	101.4	41.3	328.3	51.7	15.1	28.2	190.0
	DZ//MP2/6-31G*	77.4	24.0	178.3	57.0	-13.7	5.2	117.7
	II'//MP2/6-31G*[d]		20.5	178	52.7	-14.0	3.3	115.4
	II//MP2/6-31G*[d]		20.4	177	52.9	-13.4	3.5	115.0
	DZ/MP2/6-31G**	76.9	23.0	174.2	55.1	-15.9	3.6	114.7
H-bridged (2)	DZ//6-31G*		19.1	160				
	II'//6-31G*[d]		15.0	156				
	DZ//MP2/6-31G*		19.8	161.2				
	DZ//MP2/6-31G**		19.1	161.2				
	II'//MP2/6-31G*[d]		15.8	157				
	II//MP2/6-31G*[d]		15.4	156				
expt (vs TMS)[e]							21.0	171.6

[a] Angles in degrees. [b] Average values for C_1 and C_4. [c] Average values for C_2 and C_3. [d] IGLO calculations with basis II and II' by U. Fleischer. [e] Averaged values; ref 4. The ^{13}C absolute chemical shifts of CH_4 and TMS calculated with the DZ basis set differ by only 0.2 ppm.

the former becomes slightly (0.3 kcal/mol) more stable when this correction is included.

Does the MP2(fu) optimization overemphasize the degree of methyl bridging in **1**? We investigated this possibility by optimizing structures with varying degrees of bridging (the $C_2^+-C_3-C_4$ angle was fixed, and all other parameters were allowed to optimize fully at HF/6-31G*). Subsequent MP4(sdtq)/6-31G* single-point calculations show that no structure is more stable than **1** (angle $C_2^+-C_3-C_4 = 77°$).

Can differential solvation invert the relative stability of **1** and **2**? Although accumulating evidence shows that solvation has only a minor influence on relative stabilities of isomeric carbocations,[18] we investigated this possibility with the self-consistent reaction field (SCRF) method.[19] Calculations on the two minima, **1** and **2**, reveal a preferential stabilization of the *H-bridged* structure **2**. While specific solvation effects are not treated in this model, there is no basis on which to expect that these would change the relative stability.

We believe that this information is sufficient to establish the H-bridged **2** as the most stable 2-butyl cation structure. Nevertheless, additional evidence reinforces this conclusion. In an extensive investigation of carbocation structures, we have shown that chemical shifts calculated by the IGLO method[20] can be used to decide between isomers that have similar energies but different structures.[12,14b,20,21] Table II summarizes the IGLO chemical shifts calculated for **1-3**. These do not depend on the size of the IGLO basis set (DZ, II, II'). All geometries for **2** give acceptable agreement of IGLO chemical shifts vs experiment. This is not true for **1** and **3**. The classical structure (**3**) can be excluded from consideration on this basis. The chemical shifts for **1** depend strongly on the $C_4-C_3-C_2^+$ angle (Figure 2). All the fully optimized geometries of **1** (HF/3-21G, HF/6-31G*, MP2(fu)/6-31G*, and MP2(fu)/6-31G**) lead to IGLO chemial shifts that differ by over 50 ppm from experiment. Agreement with experiment can only be achieved by artificially fixing the $C_4-C_3-C_2^+$ angle to 92.5° (Figure 2). However, this geometry is 0.6 kcal/mol higher in energy than the corresponding 77° structure (at MP4sdtq/6-31G*//HF/6-31G*).

Our evidence favors the C_2 H-bridged structure (**2**) for the 2-butyl cation, although the methyl-bridged alternative (**1**) is only slightly (ca. 0.3 kcal/mol, possibly increased by small solvation differences) less stable. This conclusion agrees excellently with Saunders's findings.[5] In view of the small energy differences between the 2-butyl cation isomers, it might be possible that surface effects dominate the situation under the conditions of the Johnson-Clark measurements.[7]

Acknowledgment. The work at Erlangen was supported by the Fonds der Chemischen Industrie, the Stiftung Volkswagenwerk, and the Convex Computer Corporation. J.W.d.M.C. thanks CNPq-Brazil for financial support through a doctoral fellowship. We also thank Dr. U. Fleischer for assistance with the IGLO program, M. Saunders for constructive criticism, and D. T. Clark for extensive discussions and the suggestion that surface effects might influence the 2-butyl cation structure under the conditions of this experiment. Thanks also go to the IBM Düsseldorf Computing Center for providing significant computing resources.

Registry No. 1, 16548-59-7; **2**, 126191-46-6.

Supplementary Material Available: Table of the absolute energies of 2-butyl cation isomers (1 page). Ordering information is given on any current masthead page.

(18) (a) Saunders, M.; Chandrasekhar, J.; Schleyer, P. v. R. In *Rearrangements in Ground and Excited States*; de Mayo, P., Ed.; Academic-Press: New York, 1980; Vol. 1, Chapter 1. (b) Kirmse, W.; Zellmer, V.; Goer, B. *J. Am. Chem. Soc.* **1986**, *108*, 4912-4917.
(19) Pascual-Ahuir, J. L.; Silla, E.; Tomasi, J.; Bonaccorsi, R. *J. Comput. Chem.* **1987**, *8*, 778-787 and references cited therein.
(20) (a) Kutzelnigg, W. *Isr. J. Chem.* **1980**, *19*, 143-200. (b) Schindler, M.; Kutzelnigg, W. *J. Chem. Phys.* **1982**, *76*, 1919-1933. (c) Schindler, M. *J. Am. Chem. Soc.* **1987**, *109*, 1020-1033.
(21) Schleyer, P. v. R.; Carneiro, J. W. M.; Koch, W.; Raghavachari, K. *J. Am. Chem. Soc.* **1989**, *111*, 5475-5477, and references cited therein.
(22) Amos, R. D.; Rice, J. E. CADPAC: The Cambridge Analytic Derivatives Package, issue 4.1, Cambridge, 1989.

Differentiation of Two Stages during Establishment of Strong Metal-Support Interaction in Rh/TiO_2 Catalysts

J. P. Belzunegui, J. Sanz, and J. M. Rojo*

Instituto Ciencia de Materiales, CSIC
c/ Serrano 115 dpdo, 28006 Madrid, Spain

Received December 6, 1989

It is known that treatment under H_2 at 773 K of catalysts consisting of group VIII metals supported on TiO_2 gives rise to strong metal-support interaction (SMSI behavior),[1,2] which inhibits hydrogen adsorption on the metal. Its origin has been related to the formation of metal-titania bonding and/or to the coverage of metal by TiO_x species;[1-20] however, the nature of this phe-

(1) Tauster, S. J.; Fung, S. C.; Garten, L. R. *J. Am. Chem. Soc.* **1978**, *100*, 170-175.
(2) Tauster, S. J.; Fung, S. C.; Baker, R. T. K.; Horsley, J. A. *Science* **1981**, *211*, 1121-1125.
(3) Horsley, J. A. *J. Am. Chem. Soc.* **1979**, *101*, 2870-2874.
(4) Resasco, D. E.; Haller, G. L. *J. Catal.* **1983**, *82*, 279-288.
(5) Resasco, D. E.; Weber, R. S.; Sakellson, S.; McMillan, M.; Haller, G. L. *J. Phys. Chem.* **1988**, *92*, 189-193.
(6) Belton, D. N.; Sun, Y.-M.; White, J. M. *J. Am. Chem. Soc.* **1984**, *106*, 3059-3060.

0002-7863/90/1512-4066$02.50/0

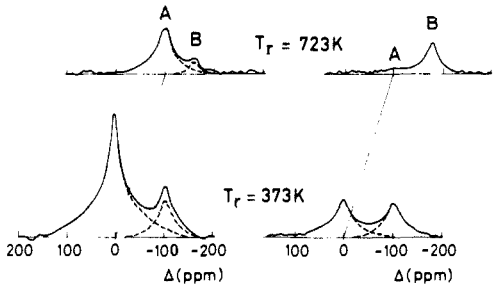

Figure 1. ^1H NMR spectra of the Rh/TiO_2 sample reduced in flowing H_2 at the indicated temperatures and then outgassed at 423 K (left) or 773 K (right). In all cases, the spectra were recorded after adsorption of H_2 (35 Torr) at room temperature.

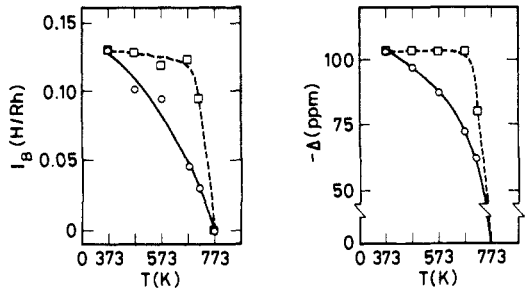

Figure 2. Effect of reduction temperature on intensity (I_B) and chemical shift (Δ) of line B. The Rh/TiO_2 sample was reduced in flowing H_2 at different temperatures and outgassed at 423 K (○) and 773 K (□) after each treatment. Represented values of I_B and Δ were measured at $p(H_2)$ = 35 Torr and room temperature.

nomenon is uncertain, and little information about the influence of the reduction degree of titania is yet available.

The catalyst Rh (2.5 wt %)/TiO_2 was prepared from $RhCl_3 \cdot 3H_2O$ by the incipient wetness method described elsewhere.[21] TEM (transmission electron microscopy) analysis revealed metal particles with sizes in the range 2–10 nm. Thermal treatments of the sample up to 773 K were performed under gas flowing in Pyrex tubular cells with high-vacuum stopcocks. The Rh/TiO_2 catalyst was first reduced in H_2 at 773 K and then oxidized in O_2 at 673 K before reduction treatments in H_2 at different temperatures. ^1H NMR spectra were recorded at room temperature with a SXP 4/100 Bruker spectrometer. The frequency used was 75 MHz.

^1H NMR spectra of an Rh/TiO_2 sample reduced in H_2 at increasing temperatures and exposed to H_2 at room temperature are shown in Figure 1. Two lines are observed: one centered at the resonance frequency (line A), assigned to protons located on the titania, and the other shifted upfield (line B) due to adsorbed hydrogen on rhodium particles.[22] In this work, the analysis

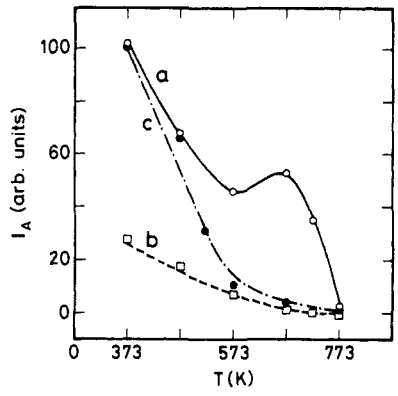

Figure 3. Plot of the intensity (I_A) of nonshifted line A against reduction temperature. The Rh/TiO_2 sample was reduced in flowing H_2 at different temperatures and outgassed at 423 K (○) and 773 K (□) after each treatment. For comparison, the intensity variation of ^1H NMR spectra of the TiO_2 sample used as support, subjected to the same reduction treatments and outgassed at 423 K, is also represented (●). Intensity values were normalized with respect to those obtained for Rh/TiO_2 and TiO_2 samples reduced at 373 K and outgassed at 423 K.

of the intensity of both lines as a function of reduction temperature has permitted evaluation of the amount of proton species on the support and the capacity of the metal to chemisorb hydrogen. In addition, chemical shift of line B has been used to follow changes in the hydrogen–metal interaction, which evidence modifications in electronic properties of the metal during SMSI establishment.

Variation of intensity (I_B) and chemical shift (Δ) of line B vs reduction temperature is shown in Figure 2. These parameters have been measured at $p(H_2)$ = 35 Torr and room temperature. That pressure was chosen because of (i) the significant amount of hydrogen adsorbed on metal particles (ca. 70% of total adsorption) and (ii) the high sensitivity of Δ to reduction treatments. In this figure, it is observed that I_B decreases with the reduction temperature in the range 373–773 K, showing the progressive establishment of the SMSI effect. The variation of Δ in this range of temperatures indicates that reduction of the support also affects the electronic properties of metal particles and modifies the hydrogen–rhodium interaction.[23] The outgassing of the sample at 773 K, after reduction treatments in the range 373–673 K, produces an increase of I_B and Δ to their initial values. In the reduction temperature range 673–773 K, the outgassing at 773 K only produces a partial recuperation in I_B and Δ values. When the sample is reduced at 773 K, line B disappears from the NMR spectrum, and the outgassing at this temperature does not modify that spectrum. Therefore, two consecutive processes, responsible for the SMSI establishment in the Rh/TiO_2 catalyst, are operating: one in the range of reduction temperature 373–673 K and the other above 673 K, which determine the reversible and irreversible character of the metal adsorption loss against the outgassing treatment.

Intensity variation of the nonshifted line (I_A) vs reduction temperature shows a progressive decrease of I_A between 373 and 573 K, which is due mainly to the surface dehydroxylation of the support, as observed for the TiO_2 sample alone (curves a and c, Figure 3). The increase of I_A, between 573 and 673 K (curve a), corresponds to incorporation of hydrogen into the support. This fact is confirmed by thermal desorption experiments on reduced samples,[24,25] in which H_2 was the principal desorbed species. From ESR and NMR results, the incorporated hydrogen was assigned[23] to hydride-like species located in oxygen vacancies at the metal–support interface. The absence of the metal prevents the incorporation of these species into the TiO_2 sample (curve c). For

(7) Belton, D. N.; Sun, Y.-M.; White, J. M. *J. Phys. Chem.* **1984**, *88*, 5172–5176.
(8) Sadeghi, H. R.; Henrich, V. E. *J. Catal.* **1984**, *87*, 279–282.
(9) Sun, Y.-M.; Belton, D. N.; White, J. M. *J. Phys. Chem.* **1986**, *90*, 5178–5182.
(10) Sanchez, M. G.; Gazquez, J. L. *J. Catal.* **1987**, *104*, 120–135.
(11) Logan, A. D.; Braunschweig, E. J.; Datye, A. K.; Smith, D. J. *Langmuir* **1988**, *4*, 827–830.
(12) Sadeghi, H. R.; Henrich, V. E. *J. Catal.* **1988**, *109*, 1–11.
(13) Beard, B. C.; Ross, P. N. *J. Phys. Chem.* **1986**, *90*, 6811–6817.
(14) Koningsberger, D. C.; Martens, J. H. A.; Prins, R.; Short, D. R.; Sayers, D. E. *J. Phys. Chem.* **1986**, *90*, 3047–3050.
(15) Martens, J. H. A.; Prins, R.; Zandbergen, H.; Koningsberger, D. C. *J. Phys. Chem.* **1988**, *92*, 1903–1916.
(16) Spencer, M. S. *J. Catal.* **1985**, *93*, 216–223.
(17) Vannice, M. A.; Hasselbring, L. C.; Sen, B. *J. Phys. Chem.* **1985**, *89*, 2972–2973.
(18) Ko, C. S.; Gorte, R. J. *Surf. Sci.* **1985**, *161*, 597–607.
(19) Levin, M.; Salmeron, M.; Bell, A. T.; Somorjai, G. A. *Surf. Sci.* **1986**, *169*, 123–137.
(20) Sheng, T.; Guoxing, X.; Hongli, W. *J. Catal.* **1988**, *111*, 136–145.
(21) Conesa, J. C.; Malet, P.; Munuera, G.; Sanz, J.; Soria, J. *J. Phys. Chem.* **1984**, *88*, 2986–2992.
(22) Sanz, J.; Rojo, J. M. *J. Phys. Chem.* **1985**, *89*, 4974–4979.
(23) Sanz, J.; Rojo, J. M.; Malet, P.; Munuera, G.; Blasco, M. T.; Conesa, J. C.; Soria, J. *J. Phys. Chem.* **1985**, *89*, 5427–5433.
(24) Munuera, G.; Gonzalez-Elipe, A. R.; Espinos, J. P.; Conesa, J. C.; Soria, J.; Sanz, J. *J. Phys. Chem.* **1987**, *91*, 6625–6628.
(25) Hongli, W.; Sheng, T.; Maosong, X.; Guoxing, X.; Xiexian, G. *Stud. Surf. Sci. Catal.* **1982**, *11*, 19–25.

reduction temperatures in the range 673-773 K (curve a), a significant decrease of I_A is observed; this variation corresponds to the elimination of previously incorporated hydride species and residual OH groups. A similar effect is also obtained by outgassing the catalyst at 773 K after each reduction treatment (curve b).

From this analysis, it is possible to differentiate two stages in the reduction of the support, which affect to different degrees the adsorption properties of the metal. In the range 373-673 K, incorporation of hydride species into the metal-support interface produces a significant decrease (63%) of hydrogen adsorption on the metal, which is recuperated by outgassing of the sample at 773 K. Above 673 K, these species are not stabilized in the support and the metal chemisorption loss must be related to other phenomena. In this case, the irreversible loss of hydrogen adsorption on the metal could be interpreted by blocking of adsorption sites with TiO_x species, as deduced from different techniques.[6-9,11,18,19,24] However, physical blocking of these sites does not explain why Δ decreases for outgassed samples, after reductions above 673 K (see dashed curve in Figure 2). For this, it is necessary to admit the presence of electronic interactions between the metal and TiO_x and/or reduced support. Moreover, the reduction of the support at high temperatures producing a significant elimination of oxygen atoms near metal particles points to the formation of rhodium-titanium bondings, not affected by outgassing treatments. In this way, the coverage of rhodium by TiO_x species should extend the metal-support interface, reinforcing our experimental observations. In summary, the NMR results reported in this work show the influence of the support reduction degree on the metal-support interaction. In particular, the incorporation of hydrogen and the formation of bondings in the metal-support interface explain the changes observed in the metal electronic properties for the two identified stages.

Acknowledgment. This research was supported by a grant from the Comisiõn Interministerial de Ciencia y Tecnología (CICYT). J.P.B. thanks the Ministerio de Educaciõn y Ciencia of Spain for a postgraduate fellowship.

Registry No. Rh, 7440-16-6; TiO_2, 13463-67-7; H_2, 1333-74-0.

{Bis(3-*tert*-butylpyrazolyl)hydroborato}zinc Alkyl Derivatives: Competitive Reactivity of Zn-C and B-H Bonds

Ian B. Gorrell, Adrian Looney, and Gerard Parkin*

Department of Chemistry, Columbia University New York, New York 10027

Arnold L. Rheingold

Department of Chemistry, University of Delaware Newark, Delaware 19716

Received February 16, 1990

We have recently described the syntheses and reactivity of the zinc[1] and magnesium[2] alkyl derivatives $\{\eta^3\text{-HB(3-Bu}^t\text{pz)}_3\}$MR (3-Bu^{t}pz = 3-$C_3N_2Bu^tH_2$; M = Zn, Mg; R = CH_3, CH_2CH_3), in which the tris(3-*tert*-butylpyrazolyl)hydroborato ligand provides a well-defined environment about the metal centers. Comparison of the reactivity of the Zn-C and Mg-C bonds in these complexes has provided good evidence for the intrinsic higher reactivity of the Mg-C vs the Zn-C bonds in isostructural derivatives. We were interested in investigating changes in reactivity at the metal center upon lowering the coordination number at the metal from 4 to 3. Here we describe the syntheses and reactivity of the three-coordinate monoalkyl zinc derivatives $\{\eta^2\text{-H}_2\text{B(3-Bu}^t\text{pz)}_2\}$ZnR (R = CH_3, CH_2CH_3, $C(CH_3)_3$).

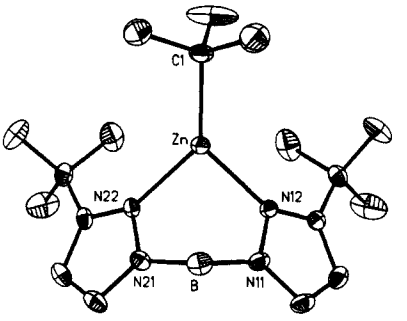

Figure 1. ORTEP diagram of $\{\eta^2\text{-B(3-Bu}^t\text{pz)}_2\}\text{ZnC(CH}_3)_3$. For clarity, thermal ellipsoids are shown at 20% probability. Selected bond distances (Å) and angles (deg): Zn-C(1) = 1.995 (7), Zn-N(12) = 2.040 (5), Zn-N(22) = 2.045 (6), N(11)-N(12) = 1.367 (8), N(21)-N(22) = 1.377 (8), B-N(11) = 1.547 (10), B-N(21) = 1.541 (12); N(12)-Zn-N(22) = 94.3 (2), N(11)-B-N(21) = 108.2 (6), C(1)-Zn-N(12) = 132.2 (3), C(1)-Zn-N(22) = 132.7 (3).

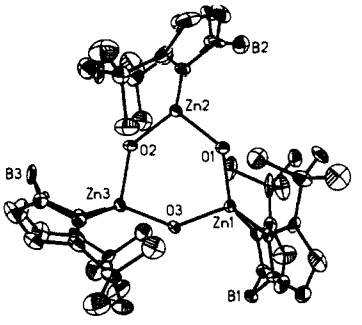

Figure 2. ORTEP diagram of $[\{\eta^2\text{-H}_2\text{B(3-Bu}^t\text{pz)}_2\}\text{Zn}(\mu\text{-OH})]_3$. For clarity, thermal ellipsoids are shown at 20% probability. Selected bond distances (Å) and angles (deg): Zn(1)-O(1) = 1.923 (8), Zn(1)-O(3) = 1.957 (10), Zn(2)-O(1) = 1.968 (9), Zn(2)-O(2) = 1.888 (9), Zn-(3)-O(2) = 1.985 (8), Zn(3)-O(3) = 1.917 (10), Zn(1)-N(12) = 2.048 (9), Zn(1)-N(42) = 2.054 (11) Zn(2)-N(22) = 2.034 (10), Zn(2)-N-(52) = 2.022 (11), Zn(3)-N(32) = 2.033 (11), Zn(3)-N(62) = 2.035 (11); O(1)-Zn(1)-O(3) = 103.6 (4), O(1)-Zn(2)-O(2) = 104.0 (4), O(2)-N(3)-O(3) = 102.0 (4), Zn(1)-O(1)-Zn(2) = 135.3 (5), Zn-(2)-O(2)-Zn(3) = 137.2 (5), Zn(1)-O(3)-Zn(3) = 137.5 (4), N(12)-Zn(1)-N(42) = 94.3 (4), N(22)-Zn(2)-N(52) = 94.4 (4), N(32)-Zn-(3)-N(62) = 93.4 (4).

Scheme I

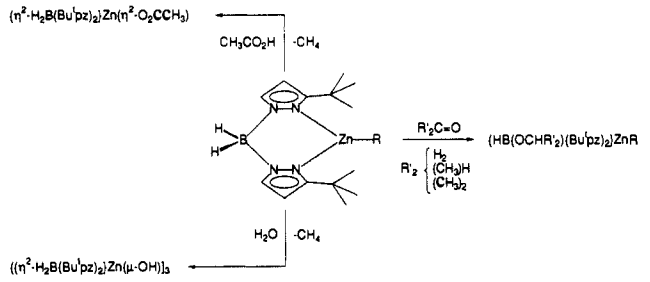

The zinc alkyl complexes $\{\eta^2\text{-H}_2\text{B(3-Bu}^t\text{pz)}_2\}$ZnR (R = CH_3, CH_2CH_3, $C(CH_3)_3$) are readily prepared by metathesis of R_2Zn with $Tl\{H_2B(3\text{-Bu}^t\text{pz})_2\}$ (eq 1). The molecular structure of the

$$R_2Zn \xrightarrow[THF]{Tl\{H_2B(3\text{-Bu}^t\text{pz})_2\}} \{\eta^2\text{-H}_2\text{B(3-Bu}^t\text{pz)}_2\}\text{ZnR} \qquad (1)$$

tert-butyl derivatives $\{\eta^2\text{-H}_2\text{B(3-Bu}^t\text{pz)}_2\}\text{ZnC(CH}_3)_3$ has been determined by an X-ray diffraction study (Figure 1), which shows that the molecule contains a distorted trigonal planar zinc center with bond angles N(12)-Zn-N(22) = 94.3 (2)°, N(12)-Zn-C(1) = 132.2 (3)°, and N(22)-Zn-C(1) = 132.7 (3)°.[3] The degree

(1) Gorrell, I. B.; Looney, A.; Parkin, G. *J. Chem. Soc., Chem. Commun.* **1990**, 220-222.

(2) Han, R.; Looney, A.; Parkin, G. *J. Am. Chem. Soc.* **1989**, *111*, 7276-7278.

(3) Crystal data for $\{\eta^2\text{-H}_2\text{B(3-Bu}^t\text{pz)}_2\}\text{ZnC(CH}_3)_3$: Monoclinic, $P2_1/n$ (No. 14), a = 14.912 (7) Å, b = 8.556 (2) Å, c = 18.482 (5) Å, β = 112.86 (3)°, V = 2173 (2) Å^3, Z = 4, ρ(calcd) = 1.17 g cm^{-3}, μ(Mo Kα) = 11.7 cm^{-1}, λ(Mo Kα) = 0.71073 Å (graphite monochromator); 4235 unique reflections with $3° < 2\theta < 52°$ were collected, of which 1948 reflections with $F_o > 6\sigma(F_o)$ were used in refinement; R = 5.54%, R_w = 6.82%, GOF = 1.21.

0002-7863/90/1512-4068$02.50/0